

Full Length Research Paper

CFD modeling of the melt spinning of poly (ethylene terephthalate) at low take-up velocities

Sengul Teke¹ and Sule Altun^{2*}

¹BUTEKOM Inc., Nilüfer, Bursa, Turkey.

²Department of Textile Engineering, Engineering and Architectural Faculty, Uludag University, Bursa, Turkey.

Accepted 23 December, 2011

In this study, a model was formulated to describe the melt spinning of Poly (ethylene terephthalate) (PET) at different quench air speeds and temperatures, mass throughputs and a low range of take-up velocities. The constitutive equations of the Newtonian model were used for modeling, which assumed the flow of polymer was viscous. To simulate the influence of the process parameters on the melt spinning process, a fiber model was used and coupled with computational fluid dynamics (CFD) calculations of the quench air flow. In the fiber model, energy, momentum and mass balance were solved for the polymer mass flow. The formulation was implemented in the Fluent Continuous Fiber Model. Numerical predictions of the model were compared with experimental data reported in the literature for PET. The take up speed, mass throughput and the temperature of melt spinning were the primary parameters of final fiber properties for both simulation and experimental results. In the simulation results, the effects of take-up speed and mass throughputs were clearly different at high take-up velocities and low mass throughputs because of viscoelastic behavior of polymers in the melt spinning. The Newtonian model was more reasonable for lower take-up speeds and higher mass throughputs.

Key words: Melt spinning, poly (ethylene terephthalate), modeling, process parameters.

INTRODUCTION

Polyester fibers, specifically poly (ethylene terephthalate) (PET), are the most commonly produced synthetic fibers worldwide. The total volume produced in 2008 was 30.3 million metric tons or 71% of worldwide manmade fiber production (Engelhardt, 2009). PET is attractive because of its low-cost of raw materials, convenient processability and excellent and tailorable performance (Reese, 2003; Jaffe and East, 2007). Moreover, the melt spinning process used for PET fiber production is clean, economical and provides both being stable fiber formation and control over the microstructure of fibers (Reese, 2003).

Melt spinning is a polymer process that can be applied to thermoplastic polymers. In melt spinning, the polymer is melted above its melting temperature, which is usually 280 to 300°C for PET, and then transported and metered

for constant mass throughput. After it is forced through spinnerets, the melt falls down through the air, starts to cool and then solidifies. Laminar cooling air is preferred to control cooling. Filaments are then passed into a take-up unit that applies a force necessary for orientation and wound up on a yarn package.

Computer simulation has become a routine practice in many fields of polymer science and technology, replacing expensive and time-consuming experiments (Ziabicki, 2001). Velocity, temperature, stress and diameter profiles of polymers can be obtained via numerical simulation. Fiber formation influenced by melt spinning dynamics is the main focus of researchers such as Ziabicki and Kedzierska (1959, 1960), Ziabicki (1961, 1976, 1985), Andrew (1959), Kase and Matsuo (1965, 1967), Shimuzu (1977) and George (1982). Therefore, using numerical methods is reasonable for analyzing melt spinning dynamics and then assuming final fiber properties (Kim et al., 2009).

In this paper, a model was formulated to describe the melt spinning behavior of (PET) with different mass

*Corresponding author. E-mail: slaltun54@gmail.com, altun@uludag.edu.tr. Fax: + 90 224 29 42 067.

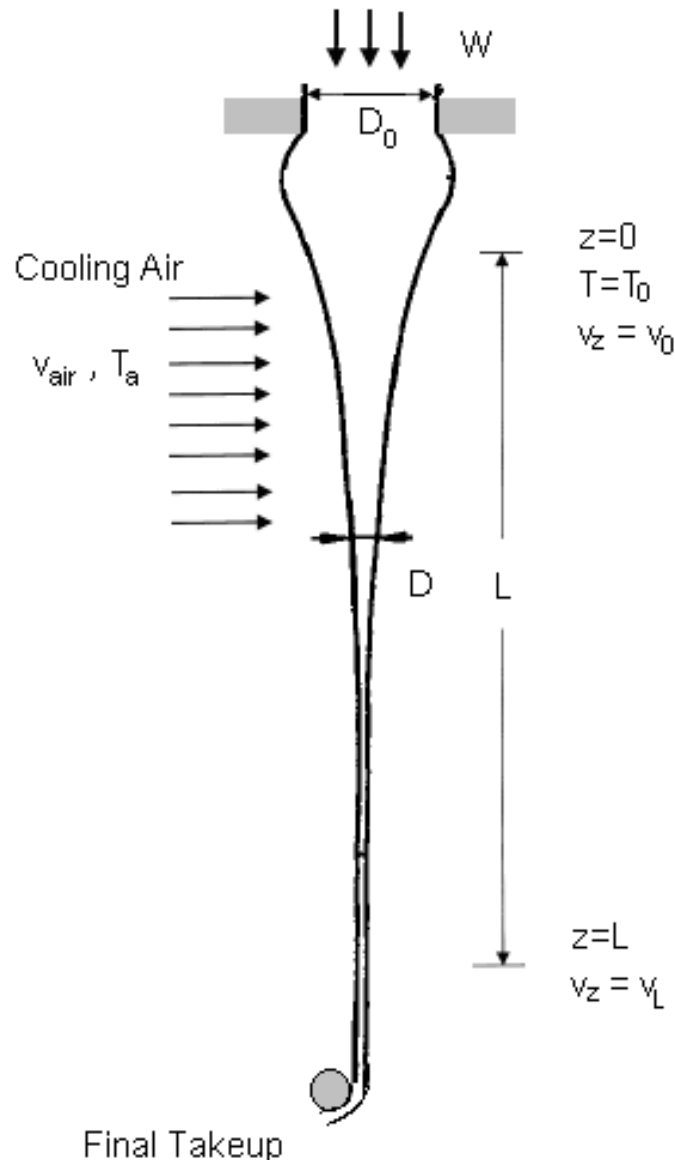


Figure 1. Physical model for melt spinning.

throughputs and a low range of take-up velocities where the degree of crystallization becomes negligible. To simulate the influence of the process parameters on the melt spinning process, a fiber model was used and coupled with computational fluid dynamics (CFD) calculations of the cooling air flow. In the fiber model, energy, momentum and mass balance equations were solved for polymer mass flow.

MODEL

The melt spinning process that is modeled in this study is shown schematically in Figure 1. In Figure 1, W is the mass throughput, D_0 is the diameter of spinneret, D_z is

the diameter of fiber, z represents the position in the axial direction of the spinline, L is the length of the spinline, T_0 is the initial temperature of the polymer, v_z is the axial velocity, v_0 is the initial axial velocity, v_L is the take-up velocity, v_{air} is the velocity of cooling air and T_{air} is the temperature of the cooling air.

Assumptions

The mathematical model was developed using the following assumptions:

1. Fibers were treated as Newtonian fluids.
2. The surface tension of the polymer/ air interface was

neglected in the equation of momentum.

3. Heat conduction along the spinline, radiant heat transfer and viscous heating were neglected in the equation of energy.
4. The heat of crystallization is ignored.
5. Radial variations in the filament cross-section are ignored to produce a one-dimensional model for the system.
6. Newtonian viscosity with Arrhenius-type temperature dependence is used.
7. The die swelling effect and the neck-like deformation are neglected.
8. The spinning of a circular monofilament is considered.

Governing equations

In melt spinning, the velocity of the liquid jet increases due to gravity and the tensile force, which is applied at the take-up point of the fibers. The conservation of mass leads to a decrease in the cross-section of the jet up to the final diameter (Doufas et al., 2000). According to our assumptions, the governing equations used in modeling are as follows:

Continuity equation

No mass is exchanged between the spinning line and the surrounding medium in melt spinning (Ziabicki, 1976; Doufas et al., 2000; Zhang et al., 2007; Patel et al., 1991):

$$W = \rho \frac{\pi D_z^2}{4} v_z \quad (1)$$

Where ρ is the polymer density and A_z is the area of the fiber.

Momentum balance

$$\frac{dF}{dz} = W \frac{dv_z}{dz} + \frac{1}{2} \rho_{\text{air}} C_f v_z^2 \pi D_z - A_z \rho g \quad (2)$$

The term on the left side of Equation (2) is the specific tensile force on the filament. The terms on the right side of Equation (2) are the inertial, air drag and gravitational forces, respectively. In Equation (2), ρ_{air} represents the density of air and g is the acceleration of gravity. In Equation (2), C_f is the air drag coefficient. The empirical correlation proposed by Matsui (1976) and Gould et al. (1980), which is widely preferred for simulating melt spinning, is used (Ziabicki et al., 1998):

$$C_f = 0.37(\text{Re})^{-0.61} \quad (3)$$

Where $\text{Re} = \frac{v_z D_z}{\nu_{\text{air}}}$ is the Reynolds number and ν_{air} is the local kinematic viscosity of air.

Energy balance

$$\rho C_p v_{\text{air}} \frac{dT_z}{dz} = -\frac{4}{D_z} \alpha (T_z - T_{\text{air}}) \quad (4)$$

Where C_p is the specific heat capacity of polymer and α is the heat transfer coefficient of polymer, which is based on a model by Kase and Matsuo (1965, 1967):

$$\alpha = 0.42 \lambda_{\text{air}} v_{\text{air}}^{-0.334} D_z^{-0.666} v_z^{0.334} \left[1 + \left(8 \frac{v_{\text{air}}}{v_z} \right) \right]^{0.167} \quad (5)$$

λ_{air} is the thermal conductivity of air in Equation (5).

Rheological constitutive equation

In the elongational flow of Newtonian fluids, the elongational viscosity (Trouton viscosity) is related to the zero-shear viscosity by a factor of three. This approach is applied to present study, only zero-shear viscosity is described (Fluent, 2006). The constitutive equation for a Newtonian fluid is as follows (Riande et al., 2000):

$$F = \eta A_z \left(\frac{dv_z}{dz} \right) \quad (6)$$

The elongational viscosity of PET was assumed to be only a function of temperature (Shimizu et al., 1985):

$$\eta = 0.73 \exp \left(\frac{5300}{T + 273} \right) \quad (7)$$

In Equations (6) and (7), η is the Newtonian viscosity of the polymer.

NUMERICAL METHODS

The Fluent Continuous Fiber Model was used to determine the influence of take-up speed and mass throughput on fiber velocity, diameter, temperature and density profiles of fiber in the melt spinning process. It is based on the solution of a system of first order differential equations representing the momentum, energy and mass balance. One-dimensional approach to predict both the flow in fibers and the flow field in the spinning was used. All differential equations (Equations 1 to 7) for conservation of mass, momentum, energy, in the fiber were solved sequentially. Since the governing equations were coupled and non-linear, several iterations had to be performed to obtain a converged solution. In melt

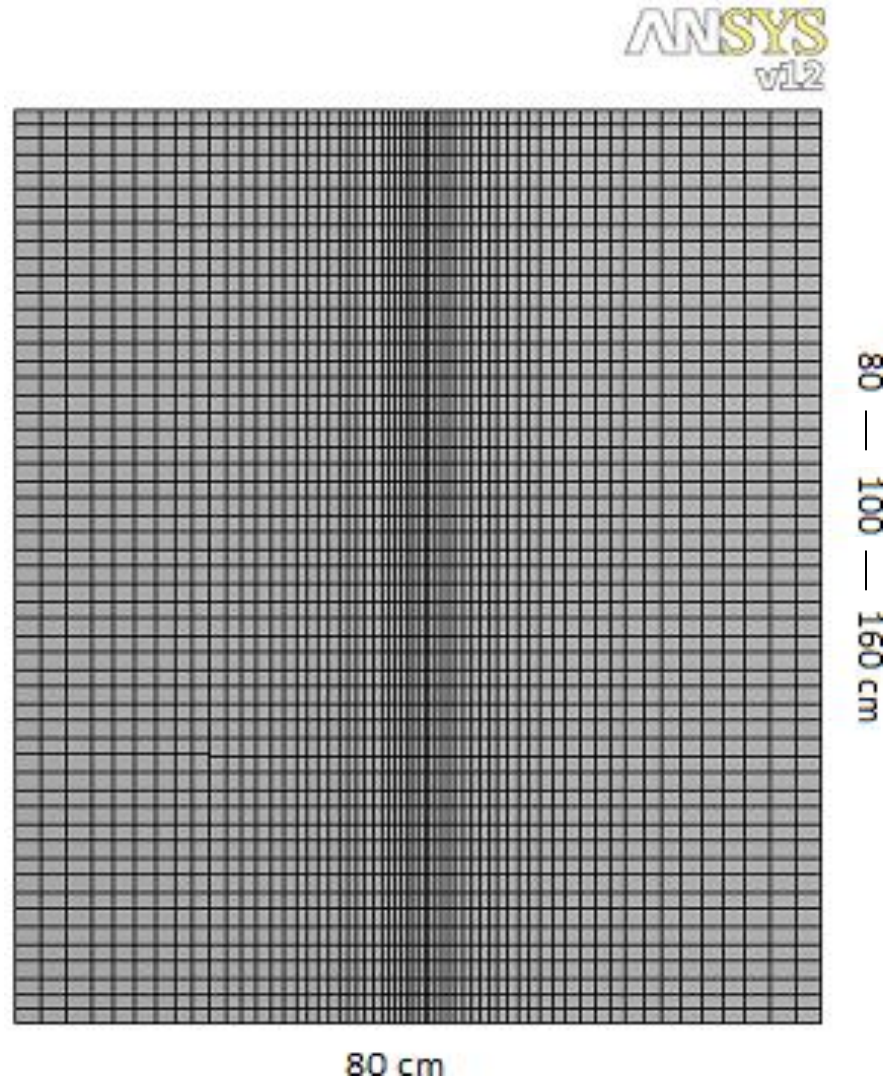


Figure 2. Mesh for cooling zone.

spinning, the fiber is considered to be liquid until its temperature falls below the solidification temperature (Fluent, 2006). The solidification temperature was 70°C, in this study. The unstructured hexahedral mesh was used in this study is shown in Figure 2. The solution procedure is based on an iterative method in which the initial rheological force is varied until the take-up velocity condition is satisfied.

Material properties

In this study, the process was modeled according to the experimental data reported in the literature for PET fibers (George, 1982; Bansal and Shambaugh, 1998). The material properties are shown in Table 1 for both sets of experimental data.

Boundary conditions

The boundary conditions are shown in Table 2 for both sets of experimental data. In the experimental data of Bansal and

Shambaugh (1998), the PET fiber was spun in the ambient laboratory air. Therefore, the air temperature was 21°C, and there was no forced convection.

RESULTS

Effects of take-up speed on the axial velocity of fibers

Figure 3 shows the axial velocity of a fiber as a function of take-up speed. When the take-up speed increased, the axial velocity of both the experimental and simulation values increased. Both profiles also showed a similar trend. The simulated and experimental values were almost equal in 1000 m/min. However, when the take-up speed increased simulation values raised more rapidly than the experimental values. The viscoelastic behavior of polymers becomes important at high speeds such that

Table 1. The material properties from the experimental data of George (1982) and Bansal and Shambaugh (1998).

Material properties	Ref.13	Ref.25
Intrinsic viscosity, IV , dl/g	0.675	0.64
Specific heat capacity of PET, C_p , J/kgK	1251	1251
Density of PET, ρ , kg/m ³	1356	1356
Thermal conductivity of PET, λ , w/Mk	0.24	0.24
Melting Temperature of PET, T_m , °C	270	270

Table 2. The boundary conditions from the experimental data of George (1982) and Bansal and Shambaugh (1998).

Boundry conditions	Ref.13	Ref.25
Extruder temperature, T_0 , °C	300	310
Cooling air temperature, T_a , °C	14	
Cooling air velocity, v_{air} , m/s	0.54	
Spinneret diameter, D_0 , cm	0.025	0.0407
Mass throughput, W , g/min	2.5	0.8-1.5-3.0
Spinline length, L cm	150	120
Take-up velocity, v_z , m/min	1000-2000-3000	1500-2500-3500

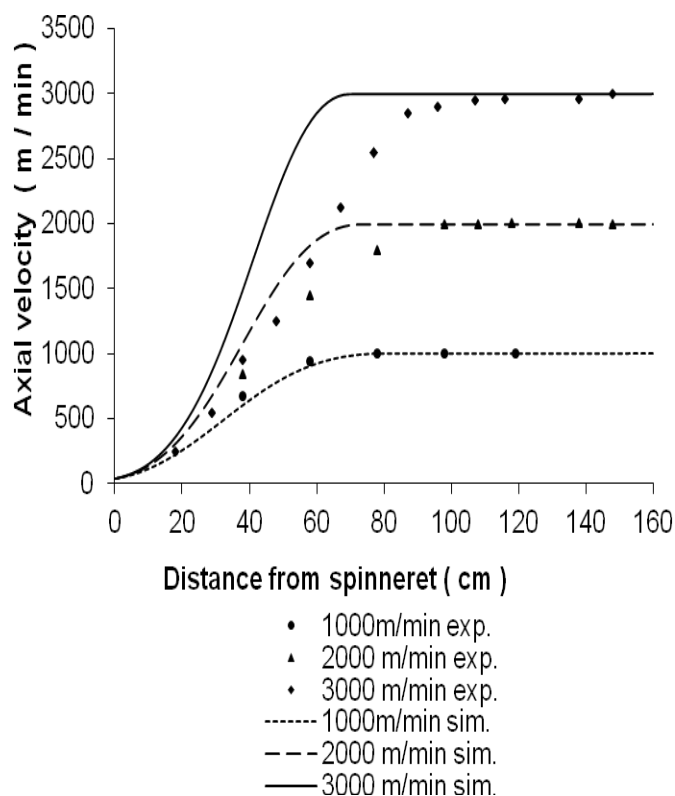


Figure 3. The axial velocity of fiber profiles for take-up speeds of 1000, 2000, 3000 m/min at constant mass throughput (2.5 g/min). The solid lines are model predictions, and symbols are the experimental data taken from George (1982).

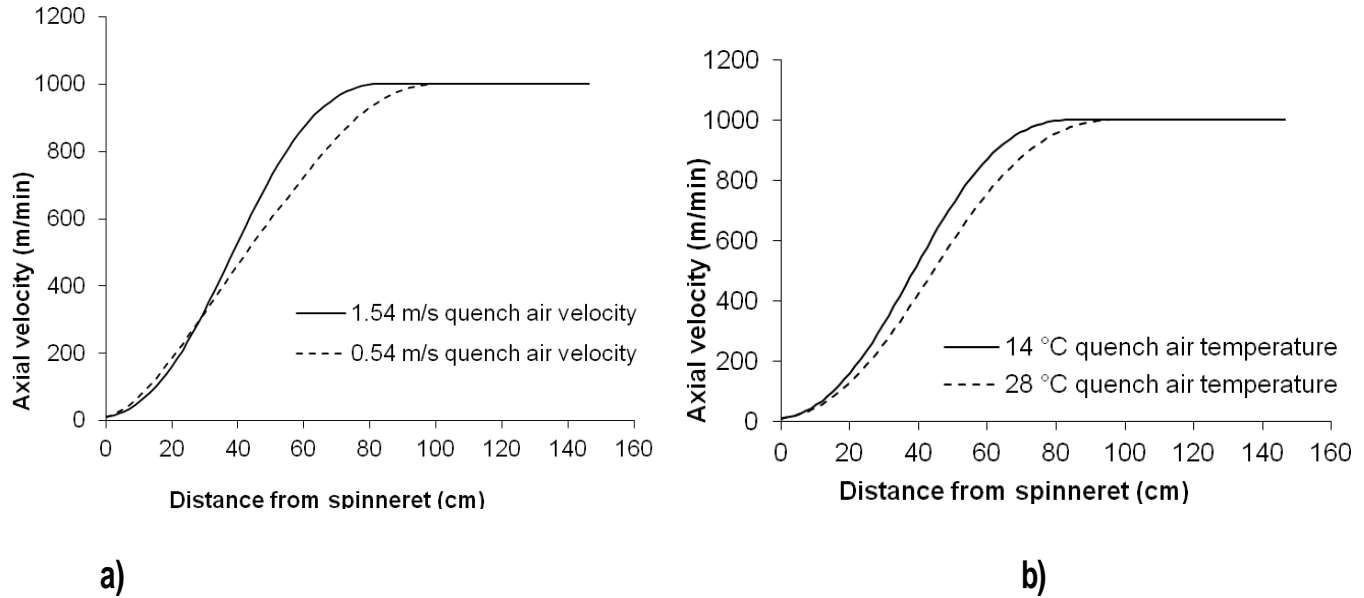


Figure 4. Simulation results. The axial velocity of fiber profiles under various cooling conditions. a) Effect of cooling air velocity and b) effect of cooling air temperature.

the Newtonian model which assumes the polymer is a viscous fluid is more reasonable at low speeds, as shown in Figure 3.

Effects of cooling air on the axial velocity of fibers

Figure 4 shows different cooling conditions of quench air temperature and air velocity on the velocity profiles. Cooling air velocity and temperature had minimum effects on the velocity, as shown in Figure 4.

Effects of mass throughput on the axial velocity of fibers

Figures 5 and 6 show the experimental and model predictions of the axial velocity of fibers at three different take-up speeds and two different mass throughputs. The axial velocity of the fiber increased quickly due to increasing take-up speed and increased slowly due to increasing mass throughput. The differences between the highest take-up speed with the lowest mass throughput and the lowest take-up speed with the highest mass throughput are shown in Figure 7.

Effects of take-up speed on the temperature of fibers

Figure 8 shows the temperature profiles of fibers as a function of various take-up speeds. The temperature of the fibers decreased along the spinline and the Newtonian molten polymer solidified slightly faster. Both

the model and the experimental data profiles showed similar trend. The variations in low take-up speed had no effect on the temperature profiles.

Effects of cooling air on the temperature of fibers

Figure 9 shows the effects of variations of the cooling conditions (quench air temperature and air velocity) on the temperature profiles. Figure 9a showed that cooling air velocity had an effect only on the curve of temperature. Figure 9b showed that, when the cooling air temperature decreased, the final fiber temperature also decreased.

Effects of mass throughput on the temperature of fibers

Figures 10 and 11 show the experimental and model predictions of the temperature of fiber with three different take-up speeds and two different mass throughputs. The effect of lower take-up speeds on the temperature profile was small. Figure 12 shows that the final temperature was higher for high mass throughputs. The Newtonian model was more reasonable for higher mass throughputs.

George (1982) and Shimuzu et al. (1985) show that, the temperature along the spinline depends only on the mass throughput and it is independent of the take-up speed. When mass throughput increased spinning stress decreased, so that the solidification point moved away

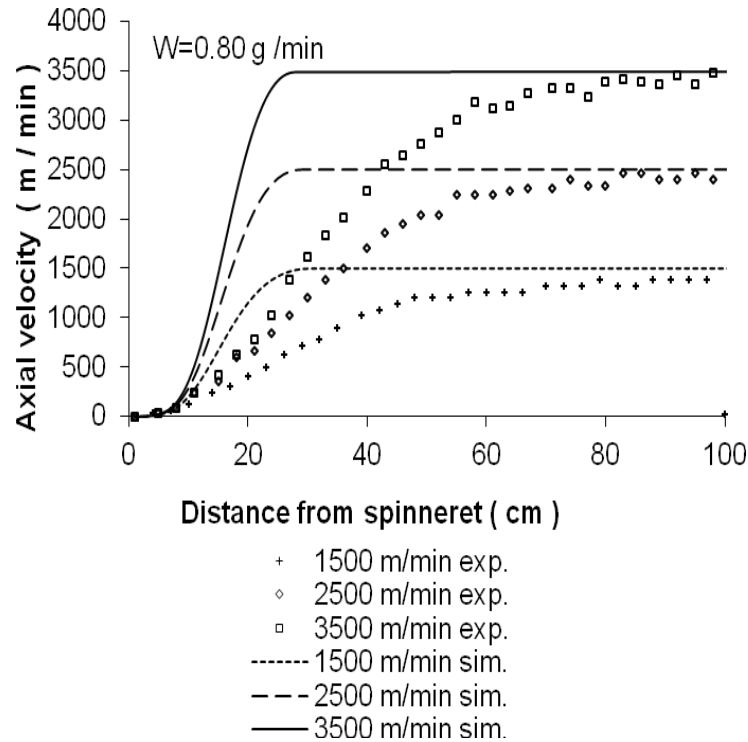


Figure 5. The axial velocity of the fiber profiles for take-up speeds of 1500, 2500, 3500 m/min at constant mass throughput (0.80 g/min). The solid lines are model predictions, and symbols are the experimental data taken from Bansal and Shambaugh (1998).

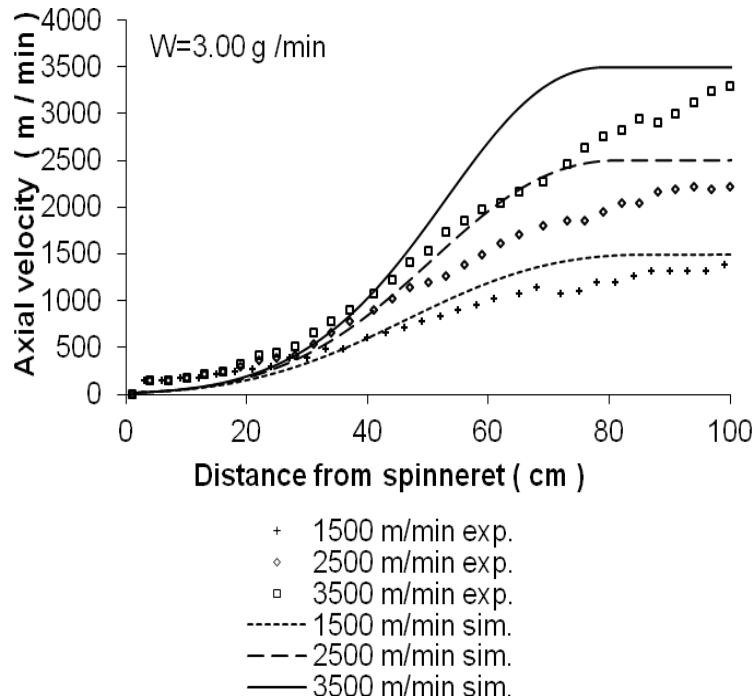


Figure 6. The axial velocity of fiber profiles for take-up speeds of 1500, 2500, 3500 m/min at constant mass throughput (3.00 g/min). The solid lines are model predictions, and symbols are the experimental data taken from Bansal and Shambaugh (1998).

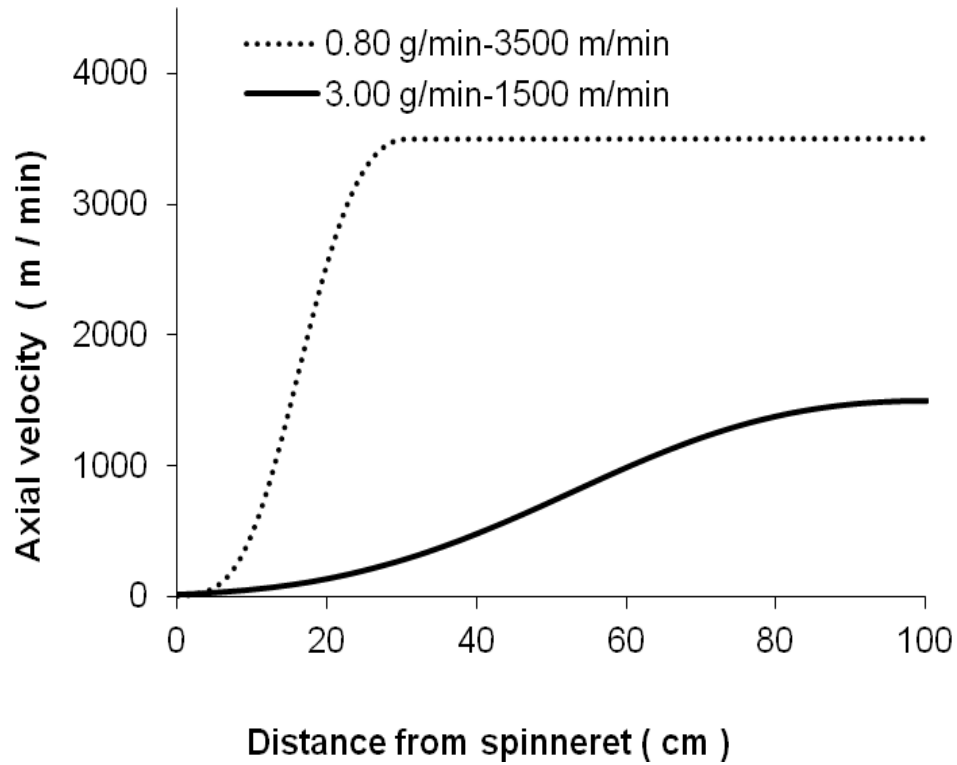


Figure 7. Simulation results. The axial velocity of fiber profiles.

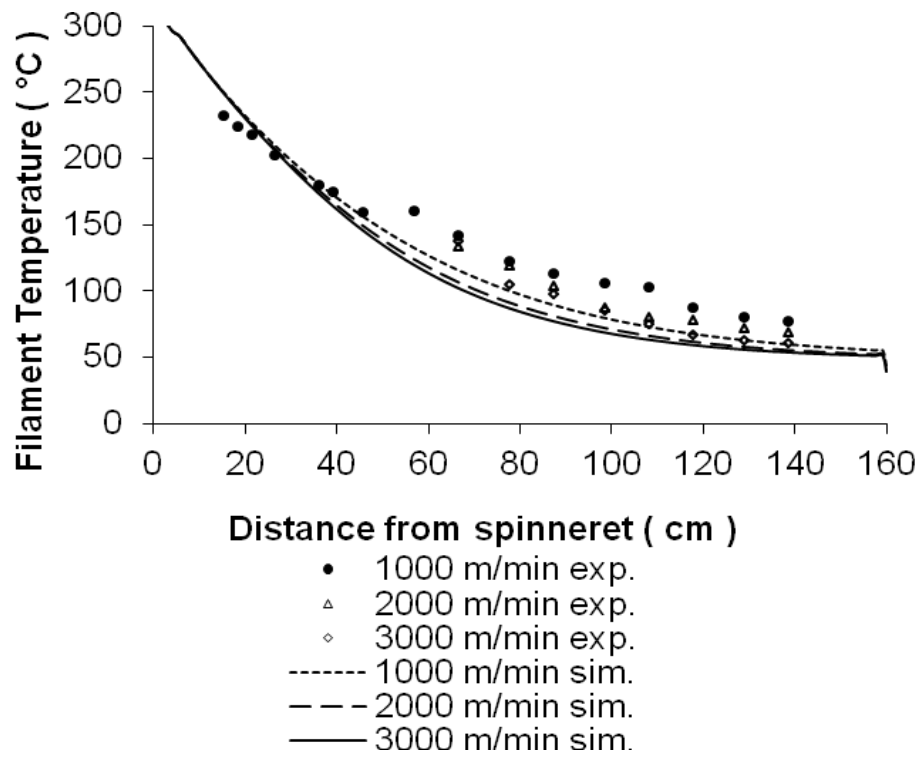


Figure 8. The temperature profiles for take-up speeds of 1000, 2000, 3000 m/min at constant mass throughput (2, 5 g/min). All the simulation conditions are summarised in the Tables 1 and 2.

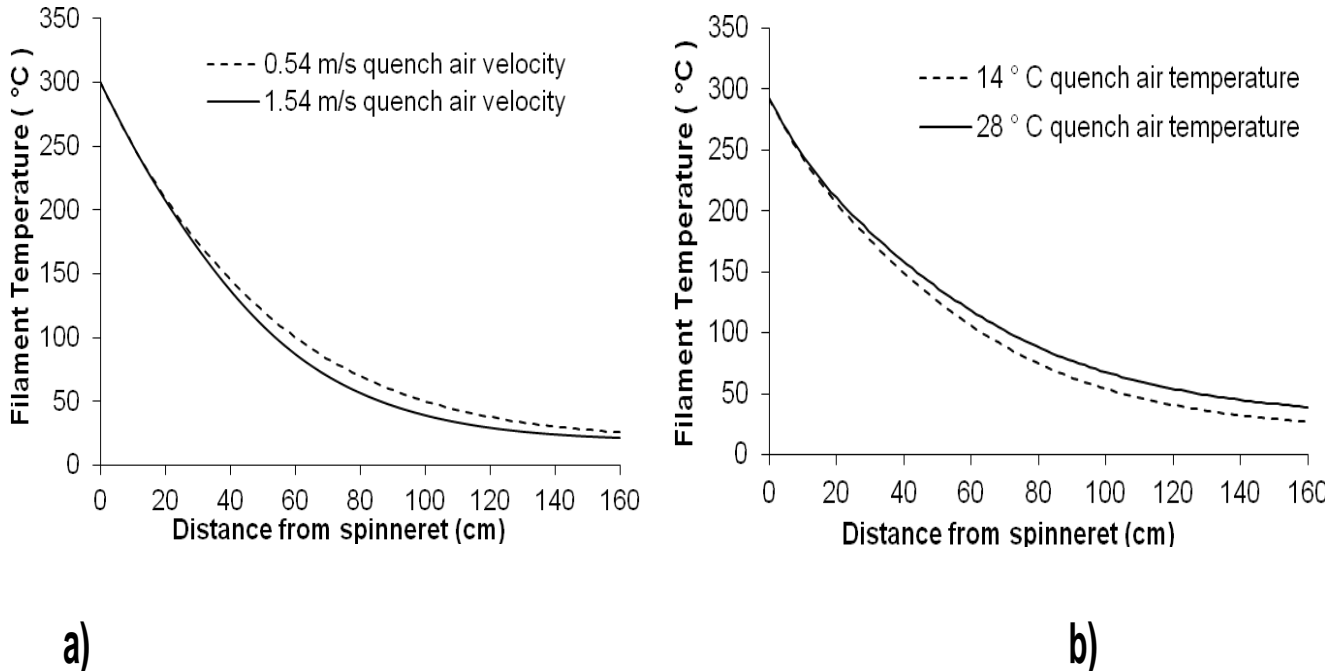


Figure 9. Simulation results. The temperature profiles for various cooling conditions. All of the simulation conditions are summarised in Tables 1 and 2. a) Effect of cooling air velocity (The quench air temperature is 14 °C) and b) effect of cooling air temperature (The quench air velocity is 1.54 m/s).

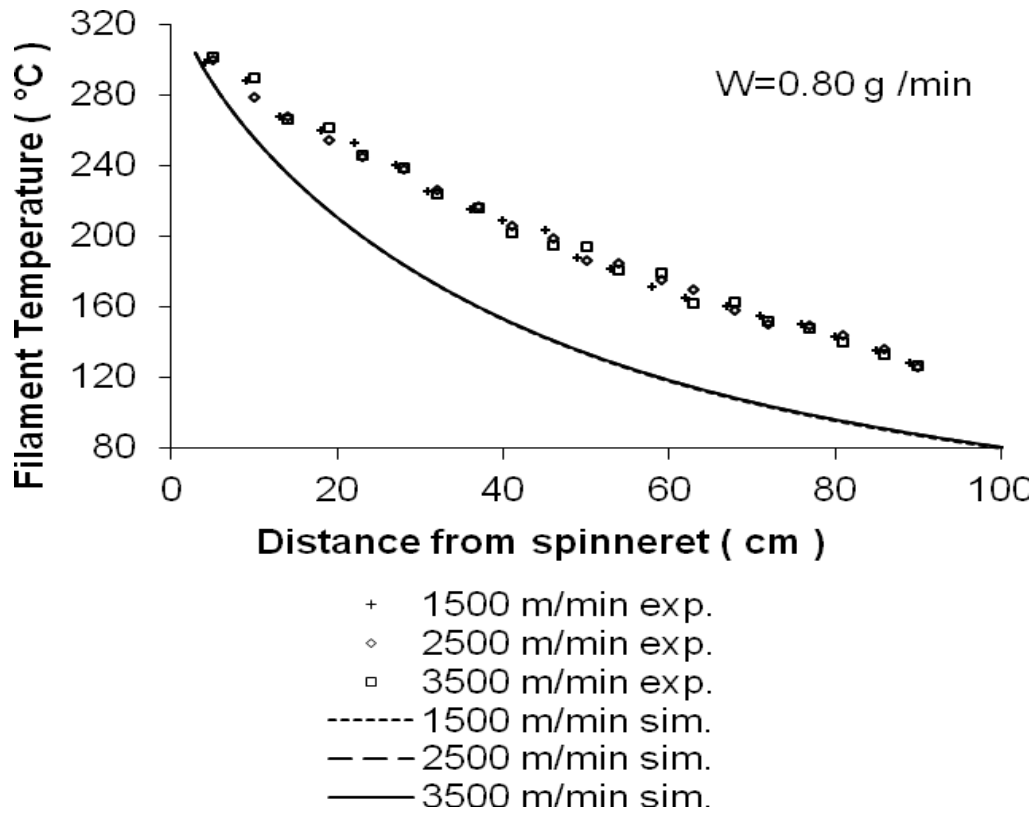


Figure 10. Temperature profiles for take-up speeds of 1500, 2500, 3500 m/min at constant mass throughput (0.80 g/min). The solid lines are model predictions and symbols are the experimental data taken from Bansal and Shambaugh (1998).

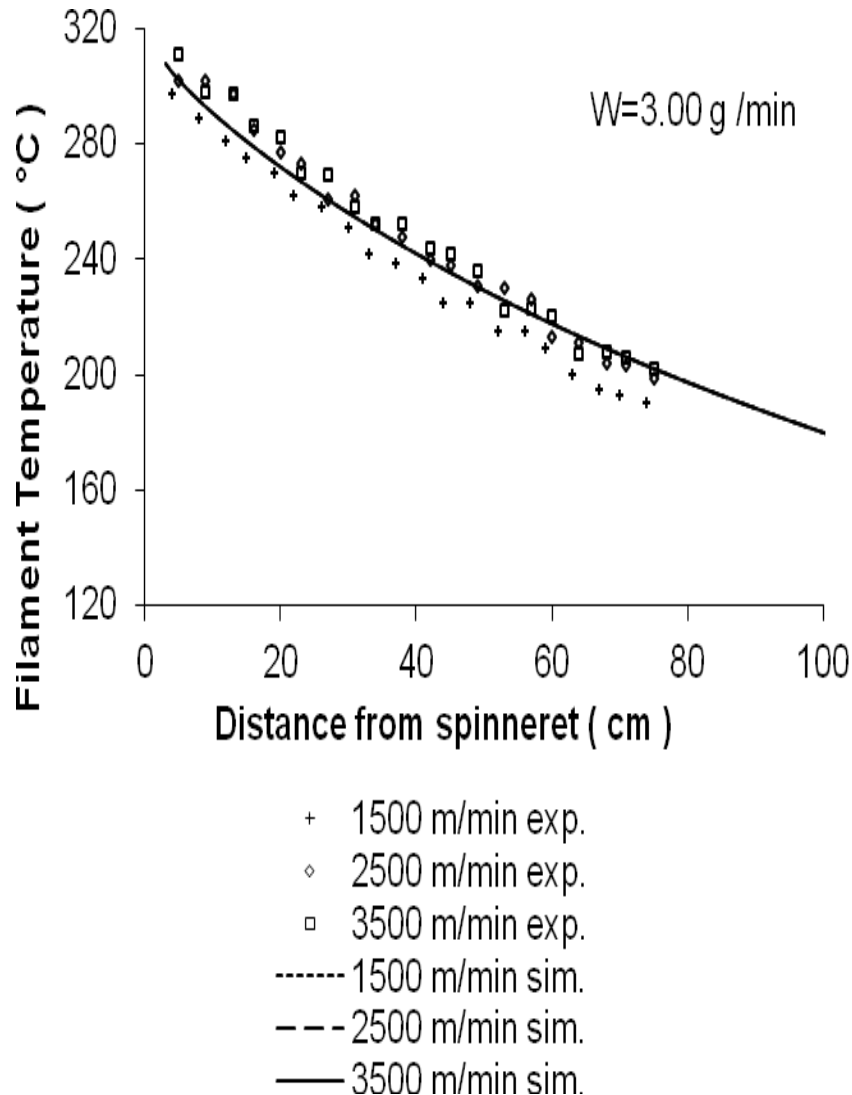


Figure 11. Temperature profiles for take-up speeds of 1500, 2500, 3500 m/min at constant mass throughput (3.00 g/min). The solid lines are model predictions, and symbols are the experimental data taken from Bansal and Shambaugh (1998).

from the spinneret.

Effects of take-up speed on the diameter of fibers

Figures 13 and 14 show the diameter profiles along the spinline for three different take-up speeds and two different mass throughputs. The diameter decreased exponentially along the spinline for both the Newtonian model and the experimental data; a similar trend was exhibited by the model. The diameter of the fibers was not significantly influenced by the take-up speed near the spinneret. As shown in Figures 13 and 14, the higher take-up speed caused a rapid decrease in the diameter.

Effects of mass throughput on the diameter of fibers

Figures 15, 16 and 17 show the effect of mass throughput on the axial fiber velocity. The solidification point moved away from the spinneret with increase mass throughput. The fiber attenuation was much slower than at lower mass throughputs.

DISCUSSION

Effects of take-up speed on the axial velocity of fibers

The trend in the graphics given in Figure 3 for both

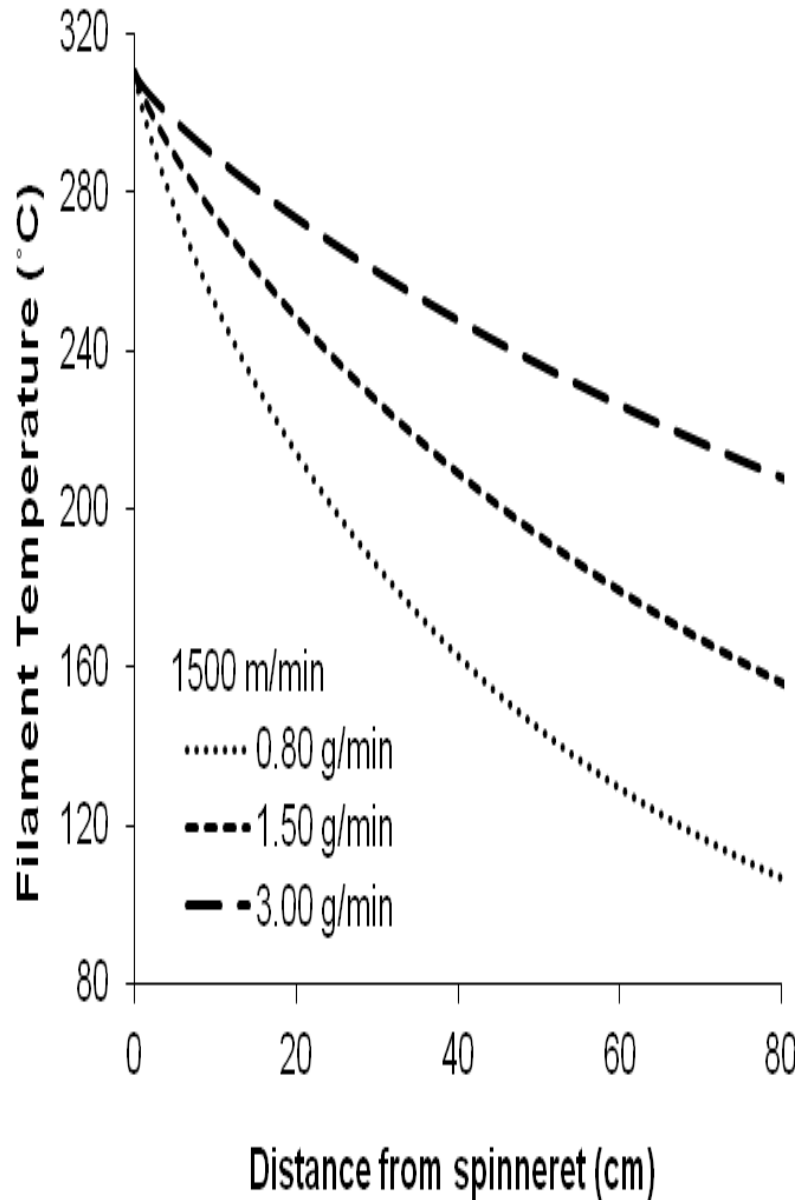


Figure 12. Simulation results. Temperature profiles for mass throughputs of 0.80, 1.50, 3.00 g/min at constant take-up speed (1500 m/min).

simulation and experimental were similar. The axial velocity of fiber increased because of increasing take-up speed. Increase in the axial velocity is due to the rheological forces. Ziabicki (1976) describes the effects of inertial and air drag forces on the rheology of polymers which influences fiber velocity. As shown in momentum balance equation (Equation 2), inertial and air drag forces increased with increasing axial velocity of fiber.

The modeling was more reasonable for the lower take-up speeds. The effect of viscosity decreases and the effect of elasticity increase on the filament attenuation by increasing take-up velocity (Beyreuther and Brunig, 2007). Therefore, the viscous behavior becomes

dominant in the elongation flow at comparatively low fiber velocities near the spinneret. However, the influence of the elastic part becomes dominant with increasing velocity (Jaffe and East, 2007).

Effects of cooling air on the axial velocity of fibers

Speed and temperature of cooling air had minimum effects on the velocity, as shown in Figure 4. When the speed of cooling air increased, elastic behavior started to become dominant. Temperature of cooling air also showed similar results. Due to viscous effects, the axial

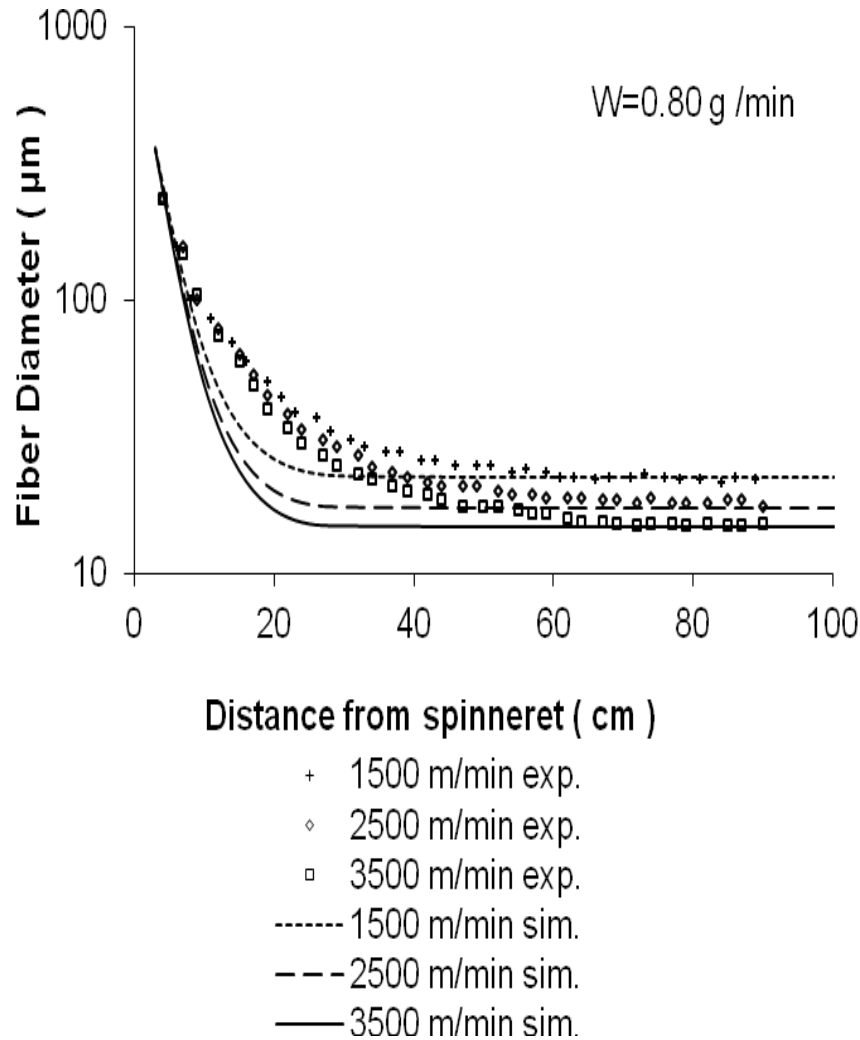


Figure 13. Diameter profiles for take-up speeds of 1500, 2500, 3500 m/min at constant mass throughput (0.80 g/min). The solid lines are model predictions, and symbols are the experimental data taken from Bansal and Shambaugh (1998).

velocity of the fibers increases quickly with increasing velocity of cooling air and slowly with decreasing temperature of cooling air.

Due to viscous effects, the axial velocity of the fibers increases quickly with increasing velocity of cooling air and slowly with decreasing temperature of cooling air.

Effects of mass throughput on the axial velocity of fibers

According to the Momentum Balance (Equation 2) the mass throughput strongly influenced the inertial forces that determine the rheological behavior of polymers. Increasing the mass throughput increases the inertial forces, such that the polymer fluid becomes more viscous. The Newtonian model was more reasonable for

higher mass throughputs to produce similar results as it is shown in Figure 6 for a take-up speed of 1500 m/min.

In Figure 7, the limits for mass throughput and take-up speed for this study are shown. The increase in the take-up velocity and the decrease in the mass throughput determine the physical limits of the process (Beyreuther and Brunig, 2007). Thus, the axial fiber velocity reaches the take-up speed faster with high take-up speed and low mass throughput as shown in Figure 7.

Effects of take-up speed on the temperature of fibers

Both the model and the experimental data profiles showed a similar trend as given in Figure 8. The variation in low take-up speed had no effect on the temperature profiles. At low take-up speeds, the material behavior is

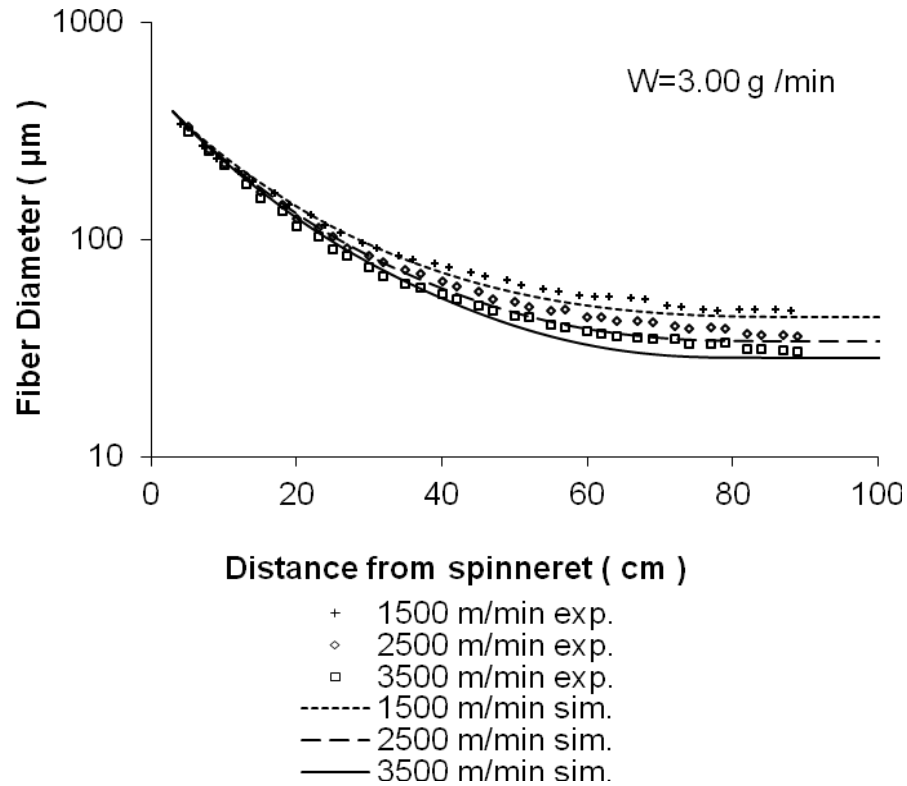


Figure 14. Diameter profiles for take-up speeds of 1500, 2500, 3500 m/min at constant mass throughput (3.00 g/min). The solid lines are model predictions, and symbols are the experimental data taken from Bansal and Shambaugh (1998).

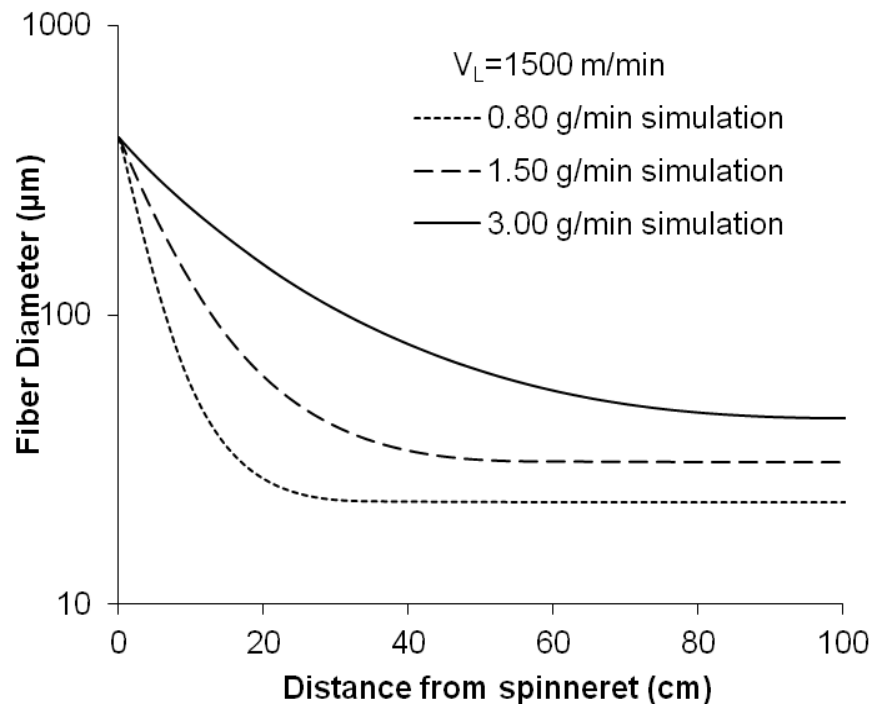


Figure 15. Simulation results. Diameter profiles for mass throughputs of 0.80, 1.50, 3.00 g/min at constant take-up speed (1500 m/min).

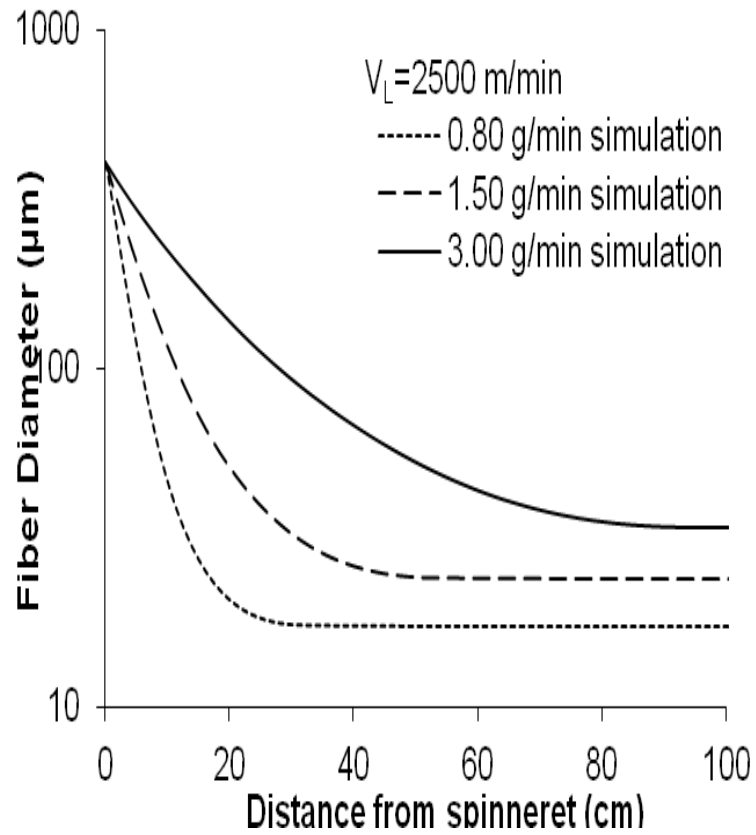


Figure 16. Simulation results. Diameter profiles for mass throughputs of 0.80, 1.50, 3.00 g/min at constant take-up speed (2500 m/min).

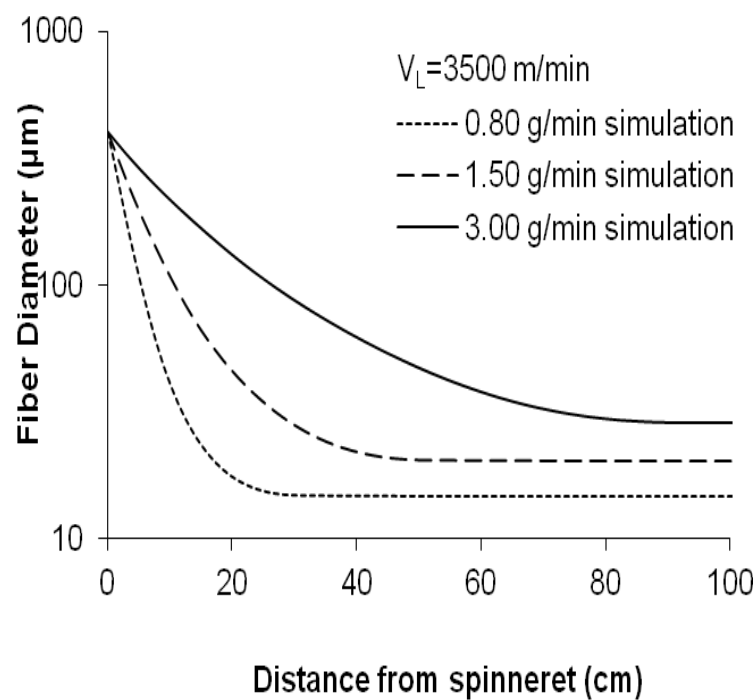


Figure 17. Simulation results. Diameter profiles for mass throughputs of 0.80, 1.50, 3.00 g/min at constant take-up speed (3500 m/min).

similar to Newtonian material, so the similar trend is reasonable.

Effects of cooling air on the temperature of fibers

When the cooling air speed increased, the fiber cooling speed also increased (Figure 9a), however the final fiber temperature did not change. The result is also compatible with Equation (4). Temperature of cooling air affects the final fiber temperature (Figure 9b). The fiber solidified quicker at same spinline length with decreasing cooling air temperature.

Effects of mass throughput on the temperature of fibers

The Newtonian model was reasonable for higher mass throughputs as given in Figures 10 and 11. According to continuity equation (Equation 1), the mass throughput affects the fiber diameter and according to energy equation (Equation 4) the fiber diameter directly influences the fiber cooling behavior. Therefore, higher fiber diameter causes slow fiber cooling at the same process conditions and the polymer becomes more viscous for a longer time.

Effects of take-up speed on the diameter of fibers

Both the model and the experimental data profiles showed a similar trend, in Figures 13 and 14. Fiber diameter variations depend on rheological forces as shown in momentum equation (Equation 2). Rheological forces cause the rapid acceleration and rapid attenuation of fiber near the spinneret. Simulation results were different from experimental results at high take up speeds because of viscoelasticity. Newtonian model is reasonable at low take up speeds for diameter modeling.

Effects of mass throughput on the diameter of fibers

The solidification point moved away from the spinneret with increase mass throughput. The fiber attenuation was slower than at lower mass throughputs, in Figures 15, 16 and 17.

Conclusions

A simulation model coupled with CFD was compared to the experimental results for melt spinning of PET fibers. Different cooling air speeds and temperatures, take-up speeds and mass throughputs were used for comparison.

Because the fibers were treated as the Newtonian fluids the results were comparable at low take-up speeds.

REFERENCES

- Andrew EH (1959). Cooling a spinning thread-line. *Brit J. Appl. Phys.*, 10: 39-43.
- Bansal V, Shambaugh RL (1998). On-line density and crystallinity of polyethylene terephthalate during melt spinning. *Polym. Eng. Sci.*, 38: 1959-1968.
- Beyreuther R, Brunig H (2007). Dynamics of fiber formation and processing modelling and application in fiber and textile industry. Springer-Verlag Berlin.
- Doufas AK, Mchugh AJ, Miller C (2000). Simulation of melt spinning including flow-induced crystallization Part I. Model development and predictions. *J. Non-Newtonian Fluid Mech.*, 92: 14-18.
- Engelhardt A (2009). Global economic slowdown shrinks world fiber consumption significantly. *IFJ*. June: 4-20.
- Fluent 6.3 (2006). Continuous Fiber Module Manual. Fluent Inc.
- George HH (1982). Model of steady-state melt spinning at intermediate take-up speeds. *Polym. Eng. Sci.*, 22: 292-299.
- Gould J, Smith FS (1980). Air drag on synthetic fiber textile monofilaments and yarns in axial flow at speeds of up to 100 meter per second. *J. Text. Inst.*, 71: 38-49.
- Jaffe M, East AJ (2007). Polyester fibers. In: Lewin M (ed) Handbook of chemistry. USA: Taylor and Francis Group, pp. 1-30.
- Kase S, Matsuo T (1965). Studies on melt spinning I. Fundamental equations on the dynamics of melt spinning. *Journal of Polym. Sci.*, 3: 2541-2554.
- Kase S, Matsuo T (1967). Studies on melt spinning II. Steady-state and transient solutions of fundamental equations compared with experimental results. *J. Appl. Polym. Sci.*, 11: 251-287.
- Kim SC, Oh TH, Han SS, Lyoo WS (2009). Effect of constitutive equations on theoretical analysis in melt spinning process. *Korea-Australia Rheol. J.*, 21: 149-153.
- Matsui M (1976). Air drag on a continuous filament in melt spinning. *Trans. Soc. Rheol.*, 20: 465.
- Patel RM, Bheda JH, Spruiell JE (1991). Dynamics and structure development during high-speed melt spinning of nylon 6 II. Mathematical modelling. *J. Appl. Polym. Sci.*, 42: 1671-1682.
- Reese G (2003). Polyester fibers: Fiber formation and end-use applications. In: Scheirs J, Long TE (eds) Modern polyesters: Chemistry and technology of polyesters and copolyesters. UK: John Wiley & Sons Ltd, pp. 401-435.
- Riande E, Callejo RD, Prolongo MG, Masegosa RM, Salom C (2000). Polymer viscoelasticity stress and strain in practice. Marcel Dekker.
- Shimizu J (1977). High-speed spinning – mechanism and fiber properties. *Kasen Geppo*, 30: 42-51.
- Shimizu J, Okui N, Kikutani T (1985). Simulation of dynamics and structure formation in high-speed melt spinning. In: Ziabicki A, Kawai H (eds) High-speed fiber spinning. John Wiley & Sons Ltd, pp. 173-200.
- Zhang CX, Wang HP, Sheng C (2007). Poly (trimethylene terephthalate) fiber melt-spinning: Material parameters and computer simulation. *Fibers Polym.*, 8: 295-301.
- Ziabicki A, Kedzierska K (1959). Studies on the orientation phenomena by fiber formation from polymer melts I. Preliminary investigations on polycapronamide. *J. Appl. Polym. Sci.*, 2: 14.
- Ziabicki A, Kedzierska K (1960). Mechanical aspects of fiber spinning process in molten polymers part II. Stream broadening after the exit from the channel of the spinneret. *Colloid Polym. Sci.*, 171: 51.
- Ziabicki A (1961). Mechanical aspects of fiber spinning process in molten polymers part III. Tensile force and stress. *Colloid Polym. Sci.*, 175: 14.
- Ziabicki A (1976). Fundamentals of fiber formation. John Wiley & Sons Interscience.
- Ziabicki A, KAWAI H (1985). "High-speed fiber spinning science and engineering aspects", Wiley-Interscience.
- Ziabicki A, Jarecki L, Wasiak A (1998). Dynamic modelling of melt spinning. *Comput. Theor. Polym. Sci.*, 8: 143-157.
- Ziabicki A (2001). Polymer crystallization in complex conditions: Towards more realistic modelling of industrial processes. *Macromol. Symposia*, 175: 225-238.